Fizykochemiczne Problemy Mineralurgii, 33 (1999), 129-141
Physicochemical Problems of Mineral Processing, 33 (1999), 129-141

J. NALASKOWSKI[*,**], J. HUPKA[***], J. D. MILLER[*]

INFLUENCE OF DISSOLVED GAS ON THE INTERACTION FORCES BETWEEN HYDROPHOBIC SURFACES IN WATER - ATOMIC FORCE MICROSCOPY STUDIES

The interaction forces between hydrophobic surfaces, the so-called hydrophobic surface forces, are important in many areas of particle separation technology, especially flotation, where the interaction between hydrophobic air bubbles and hydrophobic particle surfaces determine the efficiency of the separation process. Despite many experimental studies during the last 10 years and some theoretical analyses, there is no theory which can completely explain all experimental observations and describe the origin of these forces. One of the most successful theories to describe these hydrophobic interactions is the cavitation theory. According to this theory, long-range attraction is caused by formation of vapor/gas cavities between interacting surfaces. In the present study, the AFM colloidal probe technique was used for direct measurement of hydrophobic forces between a hydrophobic polyethylene sphere and two different hydrophobic surfaces (polyethylene and silanated silica surfaces). The influence of different gases dissolved in water was studied. Generally, long-range attractive forces between these hydrophobic surfaces and the hydrophobic PE sphere were observed. The range and magnitude of these forces were affected by the amount of gas dissolved in the system. Importantly, discontinuities in the force curves were observed which might be attributed to the formation of vapor/gas cavities between the two surfaces. These results support the cavitation theory for the origin of hydrophobic forces.

Keywords: hydrophobic surface force, atomic force microscopy (AFM), dissolved gas

INTRODUCTION

The existence of non-DLVO attractive interactions between hydrophobic surfaces, frequently much stronger than van der Waals forces and with a much longer range, has been reported in the literature (Israelachvili, 1982; Rabinovich, 1994; Yoon, 1996). This so-called hydrophobic force is important in many areas of particle separation technology, especially flotation, where differences in interaction between hydrophobic

[*] Department of Metallurgical Engineering, University of Utah, Salt Lake City, UT 84112, USA
[**] on leave from Department of Chemical Technology, Technical University of Gdansk, 80-952 Gdansk, Poland
[***] Department of Chemical Technology, Technical University of Gdansk, 80-952 Gdansk, Poland

air bubbles and hydrophobic particle surfaces are responsible for the separation process. Despite many experimental studies during last 10 years and some theoretical analyses, there is no theory which can explain all experimental observations. Some authors explain the origin of hydrophobic forces as an effect of interfacial water structure (Eriksson, 1989), or electrostatic interaction (Ruckenstein, 1991), or an effect due to the formation of cavities or nanobubbles in the interfacial region between hydrophobic surfaces (Christenson, 1988; Meagher, 1988). The last mechanism seems to be the most probable and has gained popularity in the recent literature.

During contact of two surfaces in a nonwetting liquid, a vapor cavity will form between the surfaces. The theory of such behavior was developed and discussed by Yamisky (Yaminsky, 1975; Yaminsky, 1983) and Shchukin (Shchukin, 1981). If the surfaces are sufficiently hydrophobic, cavity formation between them is energetically favorable due to the reduction of solid-liquid contact area. Recent works suggest that cavity formation also occurs before contact of the two surfaces. It is argued that, subcritical density fluctuation in the metastable liquid film will lead to cavity formation when the distance between surfaces is sufficiently small (Yaminsky, 1993). Similar results were obtained from Monte Carlo computer simulation of fluid between two hard walls (Berard, 1993) and in narrow pores (Evans, 1990). Indeed, the existence of microscopic cavities between hydrophobic surfaces has been examined experimentally by a light scattering technique (Vinogradova, 1995). Moreover, formation of cavities was found during force measurements between two hydrophobic surfaces (advancing water contact angles of 93° and 113°) using the surface force apparatus (SFA). The situation becomes even more complicated when one considers gas dissolved in water. Even by careful water degassing, it is impossible to remove traces of dissolved gases. Well-degassed water still contains about 10^{-6} mole of gas per liter, which is one order of magnitude greater than the concentration of hydrated protons in water produced by self-ionization (Gutmann, 1995). It seems quite probable that dissolved gas will influence formation of cavities between hydrophobic surfaces. It was pointed out that the concentration of gas molecules near the interacting hydrophobic surfaces might be much higher due to preferential adsorption (Yaminsky, 1993). Such expectation has been confirmed experimentally by FTIR/IRS measurements for the butane saturated water/HF treated hydrophobic silicon system (Miller, 1999). Although gas molecules are relatively small molecules, still they are much larger than the typical size of density fluctuations in pure water as predicted theoretically (Yaminsky, 1993). It is even speculated (and to some extent confirmed experimentally) that gas dissolved in water can exist in the form of stable, submicroscopic bubbles (Bunkin, 1990; Bunkin, 1993). Submicroscopic bubbles preferentially adhere to the hydrophobic surface because energetically infavourable liquid-vapor and liquid-solid interfaces are replaced by the vapor-solid interface.

It has been shown theoretically that the phase transition or cavity formation and bridging between two hydrophobic surfaces, decreases the free energy of the system, which shows up as an attraction between the surfaces (Yaminsky, 1993; Berard, 1993;

Yushchenko, 1983; Yaminsky, 1997). Such an attraction was predicted to be generally long-range and increasingly strong. In such a case, the increase in concentration of dissolved gas in the system should promote cavity formation and influence the range and magnitude of the attractive force.

The issue of dissolved gas has received relatively little attention. Earlier investigations indicated that flotation of hydrophobic mineral particles was greatly improved if hydrocarbons (from methane to butane) were used instead of air (Lin, 1974; Lin, 1975). It was also found that there was no difference in the flotation rate for different gases when collector was not added (when particles remain hydrophilic). Drzymala et al. (Drzymala, 1986; Drzymala, 1997) investigated the influence of air addition on the agglomeration of different hydrophobic particles of coal and graphite. It was found that the addition of air to the system significantly increased the agglomeration rate. Simple experiments concerning the influence of dissolved gas on the hydrocarbon emulsion stability were conducted by Karaman et al. (Karaman, 1996). The sample containing non-treated water separated completely within minutes, while that in the degassed tube remained cloudy for hours. Zhou et al. (Zhou, 1996) reported a difference in the settling rate for coal and hydrophobized (by DDAH) silica suspensions in normal and degassed water. Very little work has been done regarding the influence of dissolved gas on direct force measurements between hydrophobic surfaces. Meagher and Craig (Meagher, 1994) measured interactions between a polypropylene hemisphere and polypropylene flat surfaces in water using AFM. They reported short-range hydrophobic attraction only (up to 10 nm), but they found in degassed water that the range of interaction was slightly smaller.

EXPERIMENTAL PROCEDURE

Materials

The polyethylene (PE) used was a low-density polyethylene (Scientific Polymer Product, Inc.) with a molecular weight MW 1800 and melting point, mp. 117°C. Octadecyltrichlorosilane (OTS - 95% purity) was obtained from Aldrich. Cyclohexane (spectrophotometric grade, Mallinckrodt) was dried over freshly activated 3 ⊕ molecular sieves (Mallinckrodt). Fused silica (optical grade) plates were obtained from Harrick, Inc. Other reagents included: chloroform (spectrophotometric grade, J. T. Baker); glycerol (certified ACS grade from Fisher Scientific); ammonium hydroxide (reagent grade, Fisher Scientific); hydrogen peroxide (reagent grade, Fisher Scientific); nitrogen, argon, butane, helium (reagent grade, Mountain Airgas); and deionized water (18 $M \cdot cm^{-1}$) obtained using a Milli-Q System (Millipore).

Flat Surface Preparation

The hydrophobized silica surface was obtained by silanation in the liquid phase using octadecyltrichlorosilane (OTS). Prior to silanation silica plates were rinsed with acetone, methanol and water and then immersed in a mixture of $5H_2O$: $1H_2O_2$: $1NH_4OH$ for 25 min at 80°C. After wet cleaning, silica plates were exposed to a cold argon plasma for 30 minutes. Such cleaned silica discs were placed into Millipore water for several hours in order to establish hydroxyl groups at the silica surface. Before silanation, silica discs were dried using a stream of nitrogen. Such cleaned silica surfaces were fully wettable with water (advancing contact angle less than 3°) and no contamination was detected using optical and atomic force microscopy.

OTS solution preparation and the complete silanation process were conducted in a glove box under slight nitrogen pressure in order to avoid the presence of atmospheric water vapor in the system. A $1.01 \cdot 10^{-3}$ M OTS solution was prepared in dried cyclohexane and placed in a glass beaker (the beaker had been exposed to the OTS solution before the experiment in order to saturate the glass surface with OTS molecules and eliminate reaction with walls during silanation experiments). The beaker was placed in an ultrasonic bath filled with hexadecane (to avoid water exposure). The ultrasonic bath was cooled during silanation; a constant temperature of 24°C was maintained. The silica plates were placed on a PTFE rack and immersed in the OTS solution for 330 seconds. Then, the rack with silanated plates was removed from the OTS solution and immersed in dried cyclohexane and subsequently in a dried chloroform bath to remove excess of OTS from the surface. After that, the plates were removed from the glove box, rinsed with copious amounts of chloroform and dried in a nitrogen stream.

The polyethylene surface was prepared by melting PE at a mica surface. PE powder was placed on the freshly cleaved muscovite mica and heated to 120°C. Melted PE was pressed against mica surface using glass slide. After cooling, mica was gently removed from the PE surface and the PE surface was treated with a strong nitrogen stream in order to remove remaining mica flakes. The surface of PE was examined under optical microscope in order to assure absence of mica at the PE surface.

Colloidal Probe Preparation

Spherical polyethylene (PE) particles were obtained by melting and subsequent quenching of PE droplets suspended in glycerol. Spherical particles were filtered out using a 0.2 μm pore size disposable filter unit with a cellulose acetate membrane (Sigma Chemical Co.) and rinsed with water several times in order to remove any residual traces of glycerol. Finally, the particles were dried at room temperature in a dust free environment. Detailed procedure and characterization of PE surface after spherization is described in a previous contribution (Nalaskowski, 1999). It was found,

that the procedure only slightly affected the surface composition of PE and that a high degree of hydrophobicity (advancing water contact angle 92°) was retained.

A spherical PE particle was glued to the AFM cantilever using a technique described elsewhere (Ducker, 1991; Veeramasuneni, 1996). Tipless rectangular cantilevers (Digital Instruments, Inc.) were used. After the force measurements SEM photographs of the cantilevers were taken in order to measure the diameter of the polyethylene sphere and dimensions of the cantilever. The spring constant was calculated from the dimensions of the cantilever and was found to be 30 N/m. An SEM photograph of a typical colloidal probe as used in this work is shown on Fig. 1.

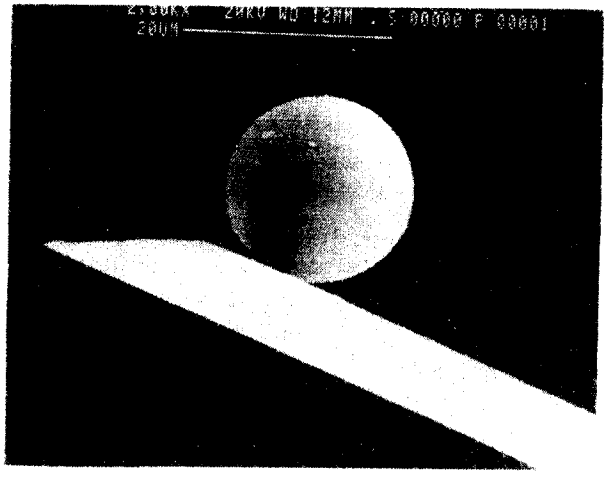

Fig. 1. SEM photograph of AFM colloidal probe

Rys. 1. Fotografia koloidalnego próbnika. Zdjęcie wykonane mikroskopem skaningowym

Gas Saturated Water Preparation

High-purity deionized water was outgassed by subsequent boiling/freezing under low pressure. Boiling/freezing cycles were repeated 4 times. 100 ml of degassed water was placed into the gas-washing bottle and gas was introduced through a coarse porous glass frit at the bottom. Gas flow of 1 l/min was maintained for 30 minutes. After the gas flow was terminated, the gas-saturated water was withdrawn with a syringe and immediately used for AFM force measurements.

Force Measurements Using AFM

Particle interaction forces were measured with a Digital Instruments Nanoscope IIIa AFM using a liquid cell. From 6 to 20 measurements were taken at different locations on each sample surface. Conversion of deflection curves to normalized force versus separation distance plots was done using AFM analysis software (Chan, 1994).

RESULTS AND DISCUSSION

Prepared PE and silanated silica surfaces exhibit a high degree of hydrophobicity determined by water contact angle measurements using the sessile drop technique. Both surfaces exhibit advancing contact angles for water of greater than 90°. See Table 1. The hysteresis between advancing and receding contact angles was greater for silanated silica, which can be explained by microheterogeneity of the silane layer, which adsorbs in a "patchy" manner. Such heterogeneity has been reported in the literature and was confirmed by AFM topographic measurements (Rabinovitch, 1994; Finn, 1994; Nalaskowski, in press). The contact angle hysteresis for the PE sample appears to be related to surface roughness due to the presence of PE crystallites at the surface. Surface roughness was determined by AFM topographic measurements (contact mode) for a 0.25 μm^2 surface region and is given in Table 1. According to the previously cited literature, strong hydrophobic attraction between the PE colloidal probe and these hydrophobic surfaces can be expected in water. Indeed, very strong and long-range attraction was found, when compared to the van der Waals force. Further, for these surfaces, a significant difference in the attractive force for outgassed and gas-saturated water was observed, both in range and magnitude of the force. The interaction forces are shown in Fig. 2 and Fig. 3. In both cases forces in outgassed water have shorter range and smaller magnitude. In the presence of helium and nitrogen saturated water, the range of the forces was greater.

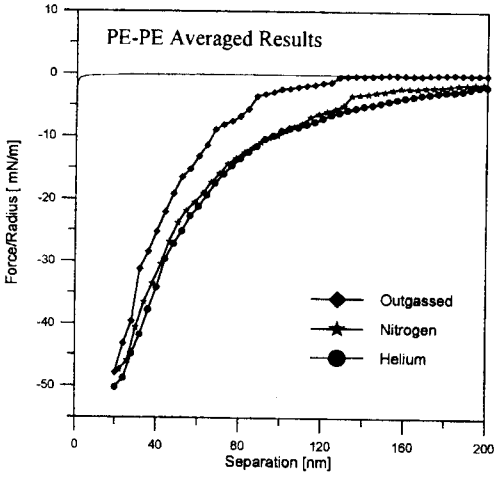

Fig. 2. Average force/radius vs. separation curves between PE colloidal probe and PE surface in outgassed and gas-saturated water. Thin solid line represents theoretical van der Waals forces for PE-PE system in water ($A=0.64 \cdot 10^{-20}$ J)

Rys. 2. Krzywe zależności średniej siły od odległości między koloidalnym próbnikiem a powierzchnią silanowanej krzemionki w warunkach nasycenia para wodną

Four gases, with different solubility in water were used in this study. The solubilities of these gases are given in Table 2 (CRC, 1992). Force curves, measured in the presence of these gases, between PE surfaces are presented on Fig. 4. Although there are differences in the magnitude and range of these forces, they do not correlate simply with the solubility of gases as might be expected. It must be admitted that each curve is the average from several measurements. During the averaging process, some

discrete features of the single measurement are lost. However, it may be visible that more step-like irregularities in the force curve are visible in the presence of more soluble gases like argon and nitrogen. The significance of these steps is discussed in the next part of this paper.

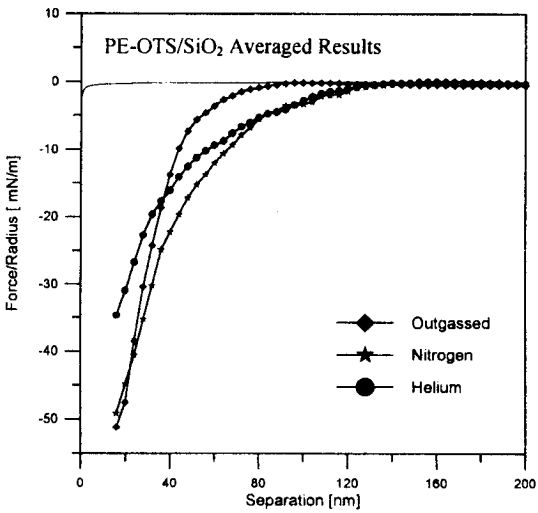

Fig. 3. Average force/radius vs. separation curves between PE colloidal probe and silanated silica surface in outgassed and gas-saturated water. Thin solid line represents theoretical van der Waals forces for PE-silica system in water ($A=0.72 \cdot 10^{-20}$ J)

Rys. 3. Krzywe zależności średniej siły od odległości między koloidalnym próbnikiem a silanowaną powierzchnią krzemionki w odgazowanej i nasyconej gazem wodzie

Tab. 1. Characterization of Polyethylene and OTS Silanated Silica Surfaces

Tab. 1. Charakterystyka powierzchni PE i silanowanej krzemionki

Surface	Advancing Water Contact Angle [deg]	Receding Water Contact Angle [deg]	Mean Roughness [nm]
Polyethylene	92	77	1.278
OTS silanated silica	94	70	0.687

Tab. 2. Solubility of Used Gases in Water at 20°C

Tab. 2. Rozpuszczalność użytych gazów w wodzie w temperaturze 20°C

Gas	Solubility in Water[ml/l]
Argon	34.2
Butane	33.4
Nitrogen	15.8
Helium	8.6

Some previously cited theoretical works (Berard, 1993; Yaminsky, 1997) predict discontinuities in the force curve during cavity formation between two surfaces. Since force is the first derivative of the free energy, rapid change of the free energy due to phase transition between surfaces implies that a discontinuity, or a step, in the force

curve should occur. These steps may be proof of cavity formation between two interacting surfaces. Experimental evidence of such steps on the force curve has been reported in only one paper (Parker, 1994), related to measurements of the interaction force between glass surfaces rendered hydrophobic (advancing contact angle 110°, receding 90°) by reaction with fluorocarbon chlorosilanes. Measurements, using a modified surface force apparatus revealed single and multiple steps on the force curve during the approach of the two surfaces which again supports cavity formation before contact. The authors concluded that it was related to the formation of submicrocavities (neck diameter approx. 50 nm) and bridging of the surfaces and suggested that this phenomenon is responsible for long-range hydrophobic attraction.

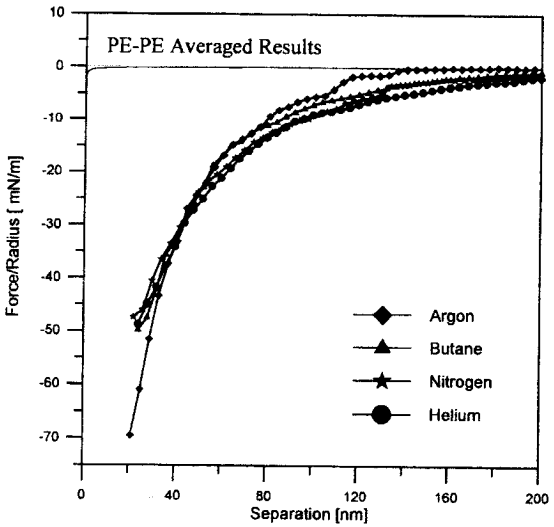

Fig. 4. Average force/radius vs. separation curves between PE colloidal probe and PE surface in water saturated with different gases. Thin solid line represents theoretical van der Waals forces for PE-PE system in water ($A=0.64\cdot10^{-20}$ J)

Rys. 4. Krzywe zależności średniej siły od odległości między koloidalnym próbnikiem a powierzchnią PE w wodzie nasyconej różnymi gazami

Figures 5, 6 and 7 show single measurements between PE surfaces in the presence of argon, nitrogen and helium saturated water, respectively. The multiple discontinuities on the force curves are clearly visible in the case of argon, they are smaller and less pronounced in the presence of nitrogen and were not present at all in helium-saturated water. The range of cavity formation suggests that first gas/vapor cavity bridging between surfaces occurs at distances from 100 to 140 nm. Multiple cavities are possible as can be seen from Fig. 5. It should be noted that cavity formation seems to be an accidental event to some extent. See Fig 6. In cases where a discontinuity in the force curve was not observed, the measured range of interaction was much greater. Thus, the presence of visible discontinuities does not to seem be necessary to observe the long-range attractive force. See Fig. 7. In this case distinct steps on the force curve between PE surfaces were not observed for helium but still these interactions are of exceptionally long range.

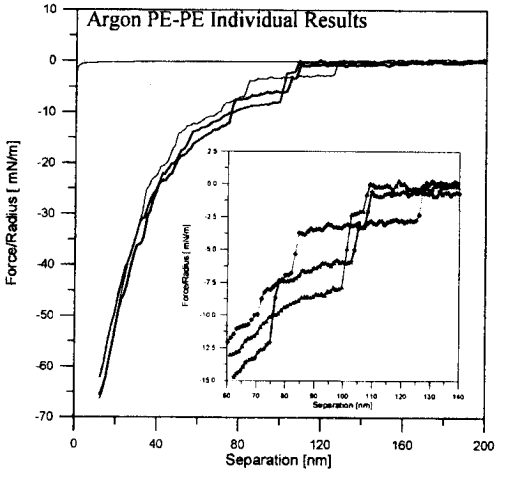

Fig. 5. Force/radius vs. separation curves between PE colloidal probe and PE surface in argon-saturated water. Separate, single measurements are shown. Thin solid line represents theoretical van der Waals forces for PE-PE system in water ($A=0.64\cdot10^{-20}$ J). Inset shows subtle structure of discontinuities region

Rys. 5. Krzywa zależności siły od odległość i między koloidalnym próbnikiem a powierzchnią PE w wodzie nasyconej argonem

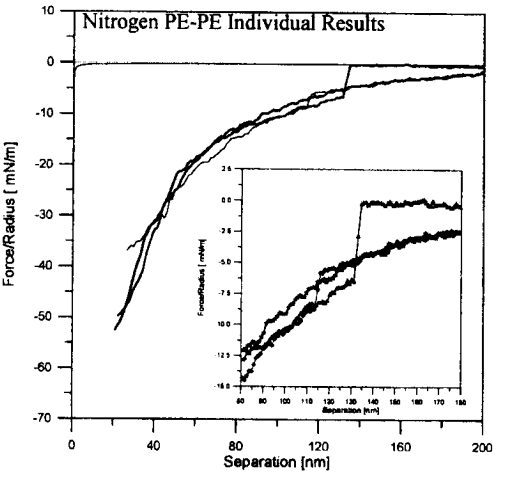

Fig. 6. Force/radius vs. separation curves between PE colloidal probe and PE surface in nitrogen-saturated water. Separate, single measurements are shown. Thin solid line represents theoretical van der Waals forces for PE-PE system in water ($A=0.64\cdot10^{-20}$ J). Inset shows subtle structure of discontinuities region

Rys. 6. Krzywe zależności siły od odległości między koloidalnym próbnikiem a powierzchnia PE w wodzie nasyconej azotem

Figures 8 and 9 show individual force measurements between the PE probe and the silanated silica surface. Very pronounced steps were also visible in these cases. In nitrogen-saturated water, single steps appear at distances from 60 to 160 nm. See Fig. 8. Interestingly, measurement without steps was also noted. The long-range attraction is similar to that observed at the PE surface in the presence of nitrogen. See Fig. 6. In addition, in the case of helium at the silanated silica surface (Fig. 9), discontinuities in the force curves were observed, unlike those observed at the PE surface (Fig. 7). It was speculated in the literature that the presence of defects or the contact angle hysteresis (heterogeneity or roughness at the surface) could substantially increase the probability of bubble or cavity formation at the surface (Ryan, 1993). The polyethylene surface is quite rough on the microscopic scale due to the presence of PE crystallites, which can promote cavitation. For rougher surfaces, it is also probable that air will remain in curvatures of the surface during immersion of the sample into water. Also it should be noted that the silanated silica surface exhibits strong chemical heterogeneity due to the "patchy" adsorption of OTS. This surface feature may be the reason for cavity formation even in the case of helium saturated water.

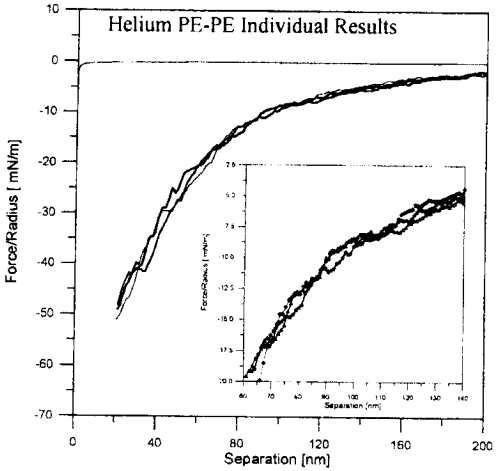

Fig. 7. Force/radius vs. separation curves between PE colloidal probe and PE surface in helium-saturated water. Separate, single measurements are shown. Thin solid line represents theoretical van der Waals forces for PE-PE system in water (A=0.64·10-20 J). Inset shows subtle structure of discontinuities region

Rys. 7. Krzywe zależności siły od odległości między koloidalnym próbnikiem a powierzchnią PE w wodzie nasyconej helem

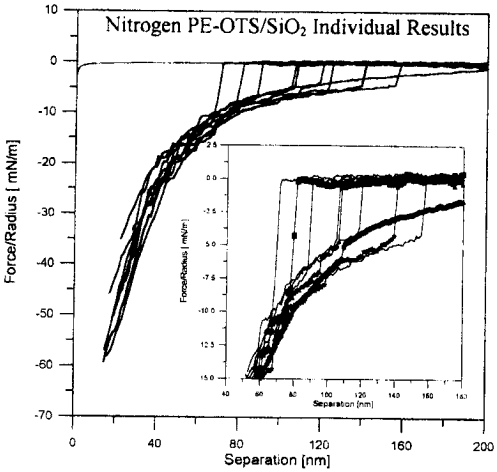

Fig. 8. Force/radius vs. separation curves between PE colloidal probe and silanated silica surface in nitrogen-saturated water. Separate, single measurements are shown. Thin solid line represents theoretical van der Waals forces for PE-silica system in water ($A=0.72\cdot10^{-20}$ J). Inset shows subtle structure of discontinuities region

Rys. 8. Krzywe zależności siły od odległości między koloidalnym próbnikiem a silanowaną powierzchnią krzemionki w wodzie nasyconej azotem

CONCLUSIONS

The influence of dissolved gas on the attractive force between hydrophobic surfaces was considered for two different systems. Although smaller and shorter attractions were observed in the absence of gas (in the outgassed water), no direct relationship between solubility of gas in water and the range or magnitude of the interactions was found. Discontinuities or steps in the force curves were found, which may indicate formation of bridging gas/vapor cavities between surfaces at distances from 60 to 160 nm. The number and range of these steps seems to be related to the solubility of gas. It is difficult to say if these cavities are composed mainly from dissolved gas or water vapor. It is important to note that long-range attractive forces were observed also in the absence of these cavities. We cannot, however, rule out the presence of very small, multiple steps in this case, which may be beyond the limit of detection. Our findings seem to support cavity formation theory and suggest the

formation of cavities between naturally hydrophobic surfaces such as PE as well as surfaces rendered hydrophobic such as silanated silica. However, it is still not clear whether the cavitation phenomena is necessary for the action of long-range hydrophobic forces in all cases.

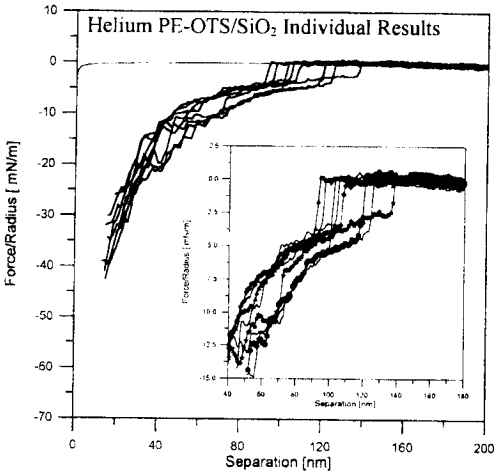

Fig. 9. Force/radius vs. separation curves between PE colloidal probe and silanated silica surface in helium-saturated water. Separate, single measurements are shown. Thin solid line represents theoretical van der Waals forces for PE-silica system in water ($A=0.72 \cdot 10^{-20}$ J). Inset shows subtle structure of discontinuities region

Rys. 9. Krzywe zależności siły od odległości między koloidalnym próbnikiem a silanowaną powierzchnią krzemionki w wodzie nasyconej helem

ACKNOWLEDGMENTS

Financial support from the US Environmental Protection Agency, National Center for Environmental Research and Quality is gratefully appreciated. Although the research described in this article has been funded partially by the US Environmental Protection Agency through grant No. R825306-01-0 to the University of Utah, it has not been subjected to the Agency's required peer and policy review and therefore does not necessarily reflect the views of the Agency and no official endorsement should be inferred. In addition support from the Basic Energy Science Division of DOE is recognized, DOE Grant No. 93-ER14315.

REFERENCES

BERARD, D. R., ATTARD, P., and PATEY, G. N., *J. Chem. Phys.*, **98** (1993) 7236
BUNKIN, N. F. and KARPOV, V. B., *JETP Lett.*, **52** (1990)18
BUNKIN, N. F., and LOBEEV, A. V., *Pis'ma Zh. Eksp. Teor. Fiz.*, **58** (1993) 91
CHAN, D. Y., University of Melbourne, Victoria, Australia, 1994
CHRISTENSON, H. K., and CLAESSON, P. M., *Science*, **239** (1988) 390
CRC Handbook of Chemistry and Physics, D. R. Lide (ed.), 1992,CRC Press

DRZYMALA, J, MARKUSZEWSKI, R., and WHEELOCK, T. D., *Intern. J. Mineral Proc.*, **18** (1986) 277
DRZYMALA, J., and WHEELOCK, T. D., *Coal Prep.* **18** (1997) 37
DUCKER, W. A., SENDEN, T. J., and PASHLEY, R. M., *Nature*, **353** (1991) 239
ERIKSSON, J. C., LJUNGGREN, S., and CLAESSON, P. M., *J. Chem. Soc. Faraday Trans.*, **285** (1989)162
EVANS, R., *J. Phys: Cond Matter*, **2** (1990) 8989
FLINN, D. H., GUZONAS, D. A., YOON, R. H., *Colloids Surfaces*, **87** (1994) 163
GUTMANN, V., AND RESCH, G., Lecture Notes on Solution Chemistry, World Scientific Publications, 1995 chapt. 10, p. 97
ISRAELACHVILI, J., and PASHLEY, R., *Nature*, **300** (1982) 341
KARAMAN, M. E., NINHAM, B. W., and PASHLEY, R. M., *J. Phys. Chem.*, **100** (1996) 15503
LIN, I. J., and METZER, A., *AIChE Symposium Series*, **71** (1975) 75
LIN, I. J., and METZER, A., *Intern. J. Mineral Proc.*, **1** (1974) 319
MEAGHER, L., and CRAIG, V. S. J., *Langmuir*, **10** (1994) 2736
MEAGHER, L., and CRAIG, V. S. J., *Langmuir*, **10** (1994) 2736
MILLER, J. D., HU, Y., VEERAMASUNENI, S., and LU, Y., *Colloids Surfaces*, to be published 1999
NALASKOWSKI, J., DRELICH, J., HUPKA, J., and MILLER, J. D., *J. Adhesion Sci. Technol.*, **13** (1999) 1
NALASKOWSKI, J., VEERAMASUNENI, S., HUPKA, J., and MILLER, J. D., *J. Adhesion Sci. Technol.*, in press
PARKER, J. L., CLAESSON, P. M., and ATTARD, P., *J. Phys. Chem.*, **98** (1994) 8468
RABINOVICH, Y. I., and YOON, R. H., *Langmuir*, **10** (1994) 1903
RABINOVICH, Y. I., and YOON, R. H., *Langmuir*, **10** (1994) 1903
RUCKENSTEIN, E., and CHURAYEV, N. V., *J. Colloid Interface Sci.*, **147** (1991) 535
RYAN, W. L., HEMMINGSEN, E. A., *J. Colloid Interface Sci.*, **157** (1993) 312
SHCHUKIN, E. D., AMELINA, E. A., and YAMINSKY, V. V., *Colloids Surfaces*, **2** (1981) 221
VEERAMASUNENI, S., YALAMANCHILI, M. R., and MILLER, J. D., *J. Colloid Interface Sci.*, **84** (1996) 594
VINOGRADOVA, O. I., BUNKIN, N. F., CHURAEV, N. V., KISELEVA, O. A., LOBEYEV, A. V., and NINHAM, B. W., *J. Colloid Interface Sci.*, **173** (1995) 443
YAMINSKY, V. V., and NINHAM, B. W., *Langmuir*, **9** (1993) 3618
YAMINSKY, V. V., *Colloids Surfaces* **129-130** (1997) 415
YAMINSKY, V. V., YUSHCHENKO, V. S., AMELINA, E. A., and SHCHUKIN, E. D., *J. Colloid Interface Sci.*, **96** (1983) 301
YAMINSKY, V. V., YUSUPOV, R. K., AMELINA, E. A., PCHELIN, V. A., and SHCHUKIN, E. D., *Kolloidn. Zh.*, **37** (1975) 918
YOON, R. H., and RAVISHANKAR, S. A., *J. Colloid Interface Sci.*, **176** (1996) 391

YUSHCHENKO, V. S., YAMINSKY, V. V., SHCHUKIN E. D., *J. Colloid Interface Sci.*, **96** (1983) 307
ZHOU, Z. A., XU, Z., and FINCH, J. A., *J. Colloid Interface Sci.*, **179** (1996) 311

Nalaskowski J., Hupka J., Miller D. J., Wpływ rozpuszczonych w wodzie gazów na siły oddziaływań między hydrofobowymi powierzchniami. Badania z użyciem mikroskopu do badań sił atomowych, *Fizykochemiczne Problemy Mineralurgii, 33 (1999), 129-141,* (w jęz. angielskim)

Siły oddziaływań między hydrofobowymi powierzchniami, nazywane hydrofobowymi siłami powierzchniowymi, są istotne w wielu procesach separacji, szczególnie w flotacji gdzie oddziaływania hydrofobowe między hydrofobowym pęcherzykiem powietrza a hydrofobową powierzchnią ziarna mineralnego determinuje efektywność tego procesu. Mimo wielu prac eksperymentalnych i teoretycznych, które zostały wykonane w ostatniej dekadzie, brak jest teorii, która w sposób całościowy wyjaśnia pochodzenie tych sił oddziaływania. Jedna z teorii, która opisuje oddziaływania hydrofobowe jest teoria kawitacji. Zgodnie z tą teoria, przyciąganie na dużej odległości jest spowodowane powstaniem gazowych kawern (cavites) między oddziaływującymi powierzchniami. Przedstawione w pracy badania zostały wykonane przy zastosowaniu techniki AFM (mikroskopu do pomiaru sił atomowych). Tę technikę użyto dla bezpośredniego pomiaru wielkości sił hydrofobowych między hydrofobową kulką polietylenu i dwoma powierzchniami ciał stałych o różnym stopniu hydrofobowości (polietylen i silanowana krzemionka). Wpływ różnych gazów rozpuszczonych w wodzie na wielkość sił oddziaływania został przebadany. Hydrofobowe siły długiego zasięgu były obserwowane dla wszystkich badanych przypadków. Zakres i wielkość tych sił był zależny od ilości rozpuszczonego gazu w wodzie. Krzywe obrazujące zmianę siły oddziaływania jako funkcję odległości, wskazują na tworzenie się gazowych kawern między dwoma powierzchniami. Otrzymane wyniki wspierają kawitacyjną teorię powstawania sił hydrofobowych.